A Hybrid Approach for Rapid Computation of Monostatic Radar Cross Section Problems with Characteristic Basis Function Method and Singular Value Decomposition

Wenyan Nie [1] and Zhonggen Wang [2*]

[1] School of Mechanical and Electrical Engineering
Huainan Normal University, Huainan, 232001, China
wynie5240@163.com

[2] School of Electrical and Information Engineering
Anhui University of Science and Technology, Huainan, 232001, China
*zgwang@ahu.edu.cn

Abstract ─ Characteristic basis function method (CBFM) is one of the effective methods to analyze wide-angle electromagnetic scattering characteristics of objects. In the general CBFM, a mass of plane waves is required to construct the characteristic basis function (CBFs) for a large-scale target resulting in a large number of CBFs. Furthermore, the accuracy cannot be further enhanced via general method by increasing the number of incident plane waves to obtain adequate CBFs. In order to alleviate these problems, a hybrid approach is proposed for fast computation of monostatic radar cross section of objects. The proposed method applies the singular value decomposition to compress the excitation matrix and introduces a new method to construct the CBFs considering the mutual interaction among blocks. Under such circumstances, the number of matrix equation solutions and the number of CBFs are both significantly reduced. Thus, the time of constructing CBFs and the complexity of reduced matrix both are reduced. Numerical examples verify and demonstrate that the proposed method is credible both in terms of accuracy and efficiency.

Index Terms ─ Characteristic basis function method, characteristic basis functions, radar cross section, singular value decomposition.

I. INTRODUCTION

The method of moments (MoM) [1] is known as an effective method to solve electromagnetic scattering problems. However, it imposes a great burden on the CPU, both in terms of computational time and memory requirement when dealing with large scale scatter problems. Fortunately, a variety of acceleration algorithms have been proposed to relieve these problems, such as the fast multipole method (FMM) [2], the adaptive integral method (AIM) [3], the multilevel fast multipole method (MLFMM) [4], the adaptive cross approximation (ACA) algorithm [5], the domain decomposition method [6, 7] and the fast dipole method (FDM) [8]. These methods have advantages in matrix-vector products (MVPs) and can handle large number of unknowns. However, most of above mentioned approaches are not appropriate for obtaining accurate monostatic radar cross section (RCS) analysis. To over this problem, many efforts have been devoted to the fast solution of monostatic RCS [9-11]. However, these methods need to use iteration method to solve liner equations which can lead to convergence difficulties when dealing with an ill-conditioned matrix.

Recently, the characteristic basis function method (CBFM) [12, 13] has been proposed that the entire scatter is divided into several blocks and each block can be solved as an independent domain. The size of the impedance matrix of the CBFM is much smaller than that of the MoM because the number of characteristic basis functions (CBFs) is smaller than the RWGs. It can be performed using the direct method for the matrix calculation; it is therefore suitable for multiple right hand-sides problem, such as monostatic RCS analysis. However, the construction of the CBFs relies on adequate incident plane waves (PWs) excited. The number of CBFs is increased with increase in the size of analysis target, which will cause more time consumption in singular value decomposition (SVD). Besides, it will be difficult to solve and store the reduced matrix directly. Under this condition, few hybrid methods have been proposed. The multilevel characteristic basis function method (MLCBFM) has been introduced in [14] to reduce the number of unknowns by applying CBFM recursively. In [15], the MLFMM is combined with the CBFM to efficiently calculate the reduced matrix. In

Submitted On: October 7, 2018
Accepted On: February 21, 2019

1054-4887 © ACES

[16], improved primary CBFs (IPCBFs) are proposed to decrease the number of the CBFs. In [17-19], the high level CBFs are calculated by fully considering the mutual coupling effects among the sub-blocks, but the total number of CBFs is increased. To some extent, these methods save time and reduce the storage requirement. However, the number of incident PWs in these methods is always overestimated and the redundant PWs will increase the calculation time both in terms of the CBFs construction and the reduced matrix calculation. In this paper, a hybrid CBFs construction method is presented. Firstly, the SVD procedure is utilized to remove the redundancy in the excitation PWs before calculating the CBFs. Secondly, the improved CBFs (ICBFs) are obtained by considering the couple effects among the blocks. Since the ICBFs contain the information of the primary CBFs (PCBFs) and the secondary level CBFs (SCBFs), the number of CBFs of each block will be reduced significantly that will further minimize the reduced matrix, hence the calculation time is also cut down. The efficiency of the proposed method is demonstrated using several examples in the paper.

II. CHARACTERISTIC BASIS FUNCTION METHOD

The CBFM divides the target into M blocks and each block is solved as an independent domain by using the CBFs [12, 13]. For each block, the CBFs can be obtained from Eq. (1):

$$\mathbf{Z}_{ii}^{e} \cdot \mathbf{J}_i^{\mathrm{CBFs}} = \mathbf{V}_i^{N_{\mathrm{pws}}} \quad (i = 1, 2, \cdots, M), \tag{1}$$

where $\mathbf{Z}_{ii}^{e}$ denotes the self-impedance of the extended block i, with dimensions of $N_i^{eb} \times N_i^{eb}$. The N_i^{eb} represents the number of unknown belonging to the extended block i and $\mathbf{V}_i^{N_{\mathrm{pws}}}$ is the excitation matrix with dimensions of $N_i^{eb} \times N_{\mathrm{pws}}$, the N_{pws} is the number of incident PWs. To eliminate the redundant information in $\mathbf{J}_i^{\mathrm{CBFs}}$ caused by overestimation, the SVD is used to reduce the redundancy of the initial CBFs. Suppose, the same number B of CBFs is obtained on each block after SVD, where B is smaller than N_{pws}, the surface current of the target can be expressed as a liner combination of these CBFs as:

$$\mathbf{J} = \begin{bmatrix} \mathbf{J}_1 \\ \vdots \\ \mathbf{J}_i \\ \vdots \\ \mathbf{J}_M \end{bmatrix} = \sum_{k=1}^{B} \mathbf{a}_1^k \begin{bmatrix} \left[\mathbf{J}_1^k\right] \\ \vdots \\ [0] \\ \vdots \\ [0] \end{bmatrix} + \cdots\cdots + \sum_{k=1}^{B} \mathbf{a}_M^k \begin{bmatrix} [0] \\ \vdots \\ [0] \\ \vdots \\ \left[\mathbf{J}_M^k\right] \end{bmatrix}, \tag{2}$$

where $\mathbf{a}_i^k$ are the unknown expansion coefficients and $\mathbf{J}_i^k$ is the kth CBFs of block i. The total number of CBFs is BM and the reduced matrix equation $\mathbf{Z}^R \boldsymbol{\alpha} = \mathbf{V}^R$ can be constructed as follows:

$$\begin{bmatrix} \mathbf{Z}_{11}^R & \mathbf{Z}_{12}^R & \cdots & \mathbf{Z}_{1M}^R \\ \mathbf{Z}_{21}^R & \mathbf{Z}_{22}^R & \cdots & \mathbf{Z}_{2M}^R \\ \vdots & \vdots & \ddots & \vdots \\ \mathbf{Z}_{M1}^R & \mathbf{Z}_{M2}^R & \cdots & \mathbf{Z}_{MM}^R \end{bmatrix} \begin{bmatrix} \boldsymbol{\alpha}_1 \\ \boldsymbol{\alpha}_2 \\ \vdots \\ \boldsymbol{\alpha}_M \end{bmatrix} = \begin{bmatrix} \mathbf{V}_1^R \\ \mathbf{V}_2^R \\ \vdots \\ \mathbf{V}_M^R \end{bmatrix}, \tag{3}$$

where the $\boldsymbol{\alpha}_i = (\mathbf{a}_i^1, \mathbf{a}_i^2, \cdots, \mathbf{a}_i^B)^{\mathrm{T}}$ represent the unknown weights of the CBFs on the block i, $\mathbf{Z}_{ij}^R$ represents the interactions between blocks i and j, and $\mathbf{V}_i^R$ is the excitation vector. The $\mathbf{Z}_{ij}^R$, $\boldsymbol{\alpha}_i$ and $\mathbf{V}_i^R$ are the sub-matrices of $\mathbf{Z}^R$, $\boldsymbol{\alpha}$ and $\mathbf{V}^R$, respectively. The $\mathbf{Z}_{ij}^R$ and $\mathbf{V}_i^R$ can be generated by using Eqs. (4) and (5):

$$\mathbf{Z}_{ij}^R = \mathbf{J}_i^{\mathrm{H}} \mathbf{Z}_{ij} \mathbf{J}_j, \tag{4}$$

$$\mathbf{V}_i^R = \mathbf{J}_i^{\mathrm{H}} \mathbf{V}_i, \tag{5}$$

where the H stands for conjugated transpose, $\mathbf{Z}_{ij}$ represents the original mutual impedance matrix between the extended block i and block j, and $\mathbf{V}_i$ is the original excitation vector. After the reduced matrix $\mathbf{Z}^R$ is generated, the unknown coefficients of the CBFs $\boldsymbol{\alpha}_i$ can be obtained by solving Eq. (3). Substituting the $\boldsymbol{\alpha}_i$ into Eq. (2), the total current distribution on the surface of the target can be obtained.

III. HYBRID CBFs CONSTRUCTION METHOD

The CBFM partly realizes the time-saving and memory requirement reduction in the calculation. However, the problem of time-consuming in CBFs construction is still existed when the size of target is increased. More importantly, for large-scale monostatic problem, the accuracy cannot be further enhanced via general method, in which the accuracy is improved by increasing the number of incident PWs to obtain adequate CBFs. Thus, a hybrid approach to solve above mentioned problems is presented.

Firstly, the redundancy information in the incident PWs is fully considered. The CBFs are solved using Eq. (1), where the incident excitation $\mathbf{V}_i^{N_{\mathrm{pws}}}$ can be described as follows:

$$\mathbf{V}_i^{N_{\mathrm{pws}}} = (\mathbf{V}_i^1(\mathbf{r}_1, \mathbf{p}_1) \cdots \mathbf{V}_i^t(\mathbf{r}_t, \mathbf{p}_t) \cdots \mathbf{V}_i^{N_{\mathrm{pws}}}(\mathbf{r}_{N_{\mathrm{pws}}}, \mathbf{p}_{N_{\mathrm{pws}}})), \tag{6}$$

where $\mathbf{r}_t$ and $\mathbf{p}_t$ represent the incident direction and polarization, respectively. $\mathbf{V}_i^t(\mathbf{r}_t, \mathbf{p}_t)$ is a matrix indicating a plane wave from a direction with a polarization. However, because the shape of each block under analysis is different, the incident PWs are usually redundant. In order to reduce the redundant PWs, the SVD is applied to deal with the excitation matrix before calculating CBFs:

$$\mathbf{V}_i^{N_{\text{pws}}} = \mathbf{U}\mathbf{W}\mathbf{V}^{\text{T}}, \tag{7}$$

where $\mathbf{U}$ and $\mathbf{V}$ are orthogonal matrices of dimensions $N_i^{eb} \times N_i^{eb}$ and $N_{\text{pws}} \times N_{\text{pws}}$, respectively. $\mathbf{W}$ is an $N_i^{eb} \times N_{\text{pws}}$ diagonal matrix and the elements of the diagonal matrix are the singular values of $\mathbf{V}_i^{N_{\text{pws}}}$. The superscript T denotes the transpose operation. Setting an appropriate threshold that typically set to be 0.001, a new set of incident excitations will be obtained retaining only those with relative singular values above the threshold. Hence, a new excitation matrix named $\mathbf{V}_i^{\text{New}}$ is obtained and the number of PWs is decreased. For the sake of simplicity, we assume that all of the blocks contain the same number K of PWs. The dimension of $\mathbf{V}_i^{\text{New}}$ is $N_i^{eb} \times K$, and K is always smaller than N_{pws}. Replacing $\mathbf{V}_i^{N_{\text{pws}}}$ in Eq. (1) with $\mathbf{V}_i^{\text{New}}$, a new equation can be constructed as follows:

$$\mathbf{Z}_{ii}^e \mathbf{J}_i^p = \mathbf{V}_i^{\text{New}}. \tag{8}$$

By solving Eq. (8), K PCBFs ($\mathbf{J}_i^p$) can be obtained on each block. The total number of matrix equation solutions is $M \cdot K$, which is smaller than $M \cdot N_{\text{pws}}$ in the CBFM as $K << N_{\text{pws}}$. Compared with the general CBFM, the time required to construct the CBFs in new method is reduced.

Secondly, the couple effects among blocks are fully consider. In [18], the SCBFs are calculated subsequently using the following equations:

$$\mathbf{Z}_{ii}^e \mathbf{J}_i^{s_1} = -\sum_{j=1(j\neq i)}^{M} \mathbf{Z}_{ij} \mathbf{J}_j^p, \tag{9}$$

$$\mathbf{Z}_{ii}^e \mathbf{J}_i^{s_2} = -\sum_{j=1(j\neq i)}^{M} \mathbf{Z}_{ij} \mathbf{J}_j^{s_1}, \tag{10}$$

where $\mathbf{J}_i^{s_1}$ and $\mathbf{J}_i^{s_2}$ represent the first-level SCBFs and the second-level SCBFs, respectively. By removing the influence of the extended part, the SCBFs $\mathbf{J}_i^{s_1}$ and $\mathbf{J}_i^{s_2}$ can be obtained by solving Eq. (9) and (10) separately. Following the above described procedure, *3K* CBFs can be obtained on each block (including K $\mathbf{J}_i^p$, K $\mathbf{J}_i^{s_1}$ and K $\mathbf{J}_i^{s_2}$). In order to further reduce the number of obtained CBFs, the ICBFs is proposed by combing the PCBFs and the SCBFs. For block *i*, the transformation is defined as follows:

$$\begin{aligned}
\mathbf{Z}_{ii}^e \mathbf{J}_i^p + \mathbf{Z}_{ii}^e \mathbf{J}_i^{s_1} + \mathbf{Z}_{ii}^e \mathbf{J}_i^{s_2} &= \mathbf{Z}_{ii}^e \left(\mathbf{J}_i^p + \mathbf{J}_i^{s_1} + \mathbf{J}_i^{s_2} \right) \\
&\equiv \mathbf{Z}_{ii}^e \mathbf{J}_i^I \\
&= \mathbf{V}_i^{\text{New}} + \mathbf{V}_i^{'} + \mathbf{V}_i^{''} \\
&= \mathbf{V}_i^{\text{New}} - \sum_{j=1(j\neq i)}^{M} \mathbf{Z}_{ij} \mathbf{J}_j^p - \sum_{j=1(j\neq i)}^{M} \mathbf{Z}_{ij} \mathbf{J}_j^{s_1},
\end{aligned} \tag{11}$$

where $\mathbf{V}_i^{'}$ and $\mathbf{V}_i^{''}$ represent the multiple scattering by the PCBFs ($\mathbf{J}_i^p$) and the SCBFs ($\mathbf{J}_i^{s_1}$) from other blocks, respectively. By solving Eq. (11), K ICBFs of block *i* can be obtained, the number of CBFs is further reduced. Furthermore, the $\mathbf{J}_i^I$ contains the information that represents the $\mathbf{J}_i^{s_1}$ and $\mathbf{J}_i^{s_2}$, so $\mathbf{J}_i^I$ can indicates the real current distribution in block *i*.

IV. NUMERICAL RESULTS

In this section, the hybrid method (CBFM-SVD) is applied to three test samples to demonstrate the accuracy and efficiency. All the targets are analyzed by multiple PWs with two modes of polarization, and All examples are carried out on a personal computer with an Inter (R) Core (TM) i5-6500 CPU with 3.2 GHz (only one core is used) and 16 GB RAM. The relative error *Err* is introduced and defined as follows:

$$Err = \left(\left\| \mathbf{I}_{\text{x}} - \mathbf{I}_{\text{MOM}} \right\|_2 / \left\| \mathbf{I}_{\text{MoM}} \right\|_2 \right) \times 100\%, \tag{12}$$

where $\mathbf{I}_{\text{MoM}}$ is the current coefficient vector computed by the FEKO, and $\mathbf{I}_{\text{x}}$ is the current coefficient vector computed by the CBFM or the CBFM-SVD. $\|\bullet\|_2$ represents the vector-2 norm.

First, the monostatic RCS of a perfect electric conduct (PEC) almond with the length of 252.374 mm at a frequency of 7 GHz is computed. There are 11564 triangular patches remained in the surface of almond after mesh subdivision and the number of unknowns is 27579. The entire almond is divided into 8 blocks. In the two methods, the number of incident PWs is set as $N_\theta = N_\phi = 20$, where N_θ and N_ϕ represent the number of incident PWs in the directions of θ and ϕ, respectively. The total numbers of CBFs and the relative error of two methods under different SVD thresholds are shown in Table 1. It can be seen that the relative error of the CBFM-SVD converges faster with reducing the SVD threshold, which proves that the CBFM-SVD has higher accuracy than CBFM because the presence of SCBFs. Taking into account the computational accuracy and computational efficiency of the two methods, the SVD threshold of the CBFM-SVD is selected as 0.005, and the SVD threshold of CBFM is selected as 0.001. The number of CBFs retained on each block and the size of reduced matrix are shown in Table 2. It can be seen that the number of CBFs and the dimensions of the reduced matrix are both decreased when the CBFM-SVD is used. In order to further illustrate the efficiency and accuracy of the proposed method, the comparison of relative error is shown in Fig. 1. It can be seen that the relative error of the CBFM-SVD converges faster with increase in the number of CBFs. The current coefficients of one arbitrary RWG basis with multiple incident angles, computed by the conventional CBFM and the CBFM-SVD are compared in Fig. 2, which are in good agreement. The

monostatic RCS in $\theta\theta$ polarization and $\phi\phi$ polarization calculated by using the CBFM and the CBFM-SVD are presented in Fig. 3 and Fig. 4, respectively. It can be seen from the figures that the results are coincided well with each other.

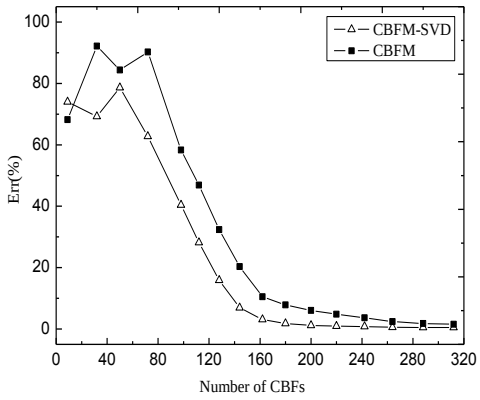

Fig. 1. The current error versus the CBFs number.

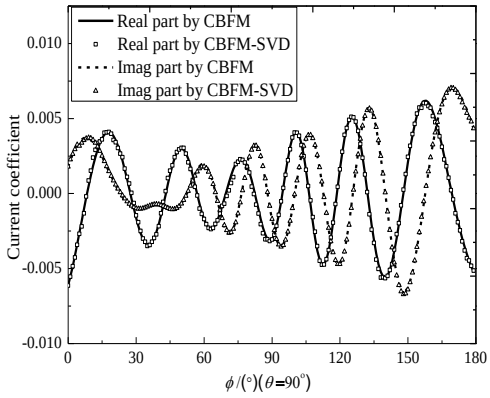

Fig. 2. Current coefficients for PEC almond.

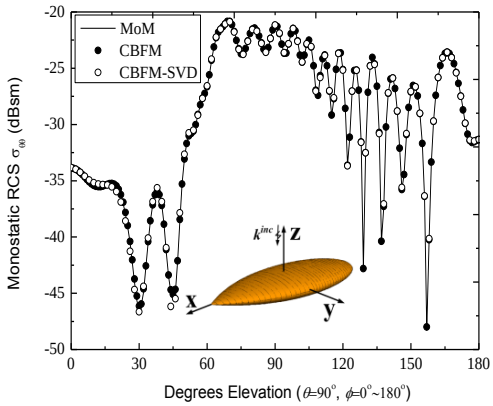

Fig. 3. The monostatic RCS of NASA in $\theta\theta$ polarization.

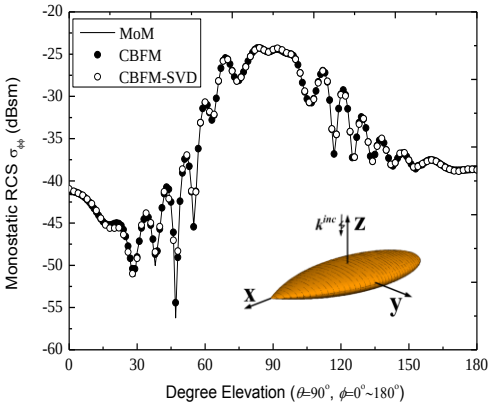

Fig. 4. The monostatic RCS of NASA in $\phi\phi$ polarization.

Then the scattering problem of a PEC cube with length of 1.2 m is presented. The frequency is 500 MHz and the cube is divided into 10 blocks. The surface of cube is discretized in 9660 triangular patches and the total number of unknowns is 24711. In the CBFM, the number of incident PWs is set as $N_\theta = N_\phi = 20$, so 800 CBFs are generated for each block and only 176 CBFs (average value) are remained via SVD. The remained CBFs are applied to construct the reduced matrix with the dimensions of 1763×1763. While in the CBFM-SVD, each block is excited by using 20 PWs in the directions of θ and ϕ. Only 127 PWs (average value) are remained resulting in 127 ICBFs for each block by using the SVD. The dimensions of reduced matrix are 1271×1271. Comparing with the CBFM, the size of matrix is further decreased. The calculation results are shown in Fig. 5 and Fig. 6, respectively. It can be seen that the results are coincided well with each other.

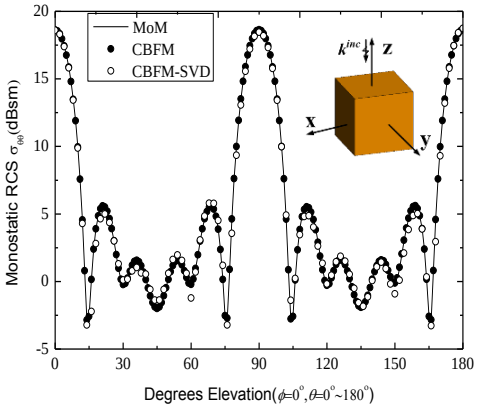

Fig. 5. The monostatic RCS of a PEC cub in $\theta\theta$ polarization.

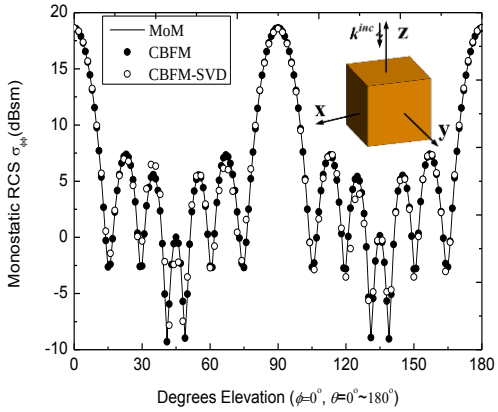

Fig. 6. The monostatic RCS of a PEC cub in $\phi\phi$ polarization.

Finally, the monostatic RCS of sixteen discrete cylinders are computed. Each cylinder has same size with height of 0.5 m and radius of 0.25 m. The frequency of incident PWs is 500 MHz and the target is divided into 16 blocks. After mesh subdivision, the surface of the objective is discretized in 20416 triangular patches and the total number of unknowns is 30624. In the CBFM, the number of incident PWs is set as $N_\theta = N_\phi = 20$. By taking advantage of SVD, the number of CBFs is reduced to 147 and the size of the reduced matrix is 2352×2352. In the CBFM-SVD, the number of incident PWs is defined as $N_\theta = N_\phi = 20$, via SVD only 111 PWs are remained resulting in 111 ICBFs for each block. In terms of the matrix size, the size of reduced matrix in the CBFM-SVD is smaller than that in the CBFM, with the dimensions of 1776×1776. The monostatic RCS in $\theta\theta$ polarization and $\phi\phi$ polarization calculated by using the CBFM and the CBFM-SVD are presented in Fig. 7 and Fig. 8, respectively. The result obtained by the CBFM-SVD agrees very well with that obtained by the CBFM.

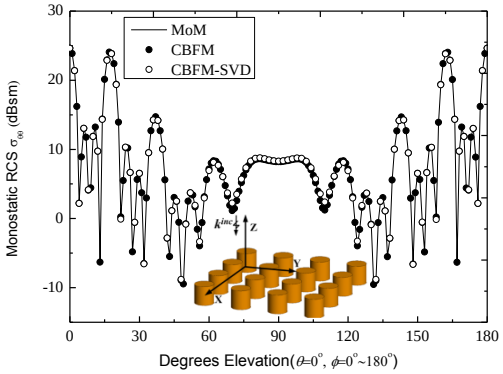

Fig. 7. The monostatic RCS of sixteen discrete cylinders in $\theta\theta$ polarization.

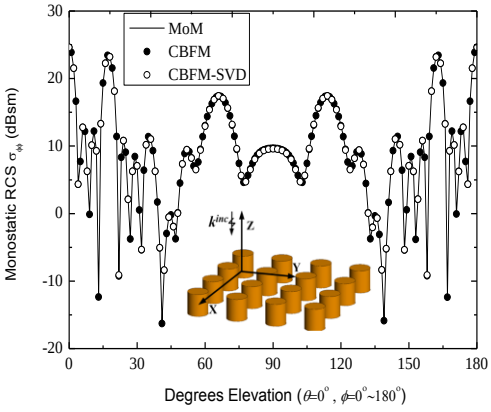

Fig. 8. The monostatic RCS of sixteen discrete cylinders in $\phi\phi$ polarization.

The calculation time of the two methods are summarized in Table 3. It can be seen that the CBFM-SVD outperforms the conventional CBFM, both in CBFs construction and in RCS computational time, the CPU time of the CBFs construction and the RCS computational time are remarkably reduced and the gains are about 38% and 22%, respectively.

VI. CONCLUSION

In this paper, a hybrid method (CBFM-SVD) is presented to efficiently compute the monostatic RCS of objects. In the proposed method, the number of required PWs has been remarkably reduced by further compression using the SVD that results in fewer matrix equation solutions. Furthermore, a novel scheme for CBFs construction is proposed by taking full consideration of the couple effects among the sub-blocks to enhance the computation accuracy. The results have validated and demonstrated that the proposed CBFM-SVD is capable of more efficiently calculating the monostatic RCS compared with the conventional CBFM without compromising the accuracy.

ACKNOWLEDGMENT

This work was supported by the Natural Science Foundation of Anhui Province under Grant No. 1808085MF166, the Anhui Provincial Key Science Foundation for Outstanding Young Talent under No. gxyq2017060, the Postdoctoral Science Foundation of Anhui Province under Grant No. 2017B214, the Overseas Visiting and Training Program for Outstanding Young Talents of Anhui Province under No. gxgwfx2018025, and the Natural Science Foundation of Anhui Provincial Education Department under Grant No. KJ2016A669.

Table 1: The total CBFs number and the relative error of two methods under different SVD threshold

SVD Threshold	CBFM		CBFM-SVD	
	Err (%)	CBFs number	*Err* (%)	ICBFs number
0.08	36.035	442	28.413	427
0.05	22.728	548	19.864	506
0.03	12.918	613	9.474	574
0.01	8.595	798	4.206	769
0.005	5.887	905	2.961	872
0.003	3.353	1073	2.323	1035
0.001	2.986	1219	2.037	1156

Table 2: The CBFs number retained on each block of two methods

Method	Block 1	Block 2	Block 3	Block 4	Block 5	Block 6	Block 7	Block 8	Size of Reduced Matrix
CBFM	124	168	185	190	180	164	130	78	1219×1219
CBFM-SVD	88	125	132	140	130	109	94	54	872×872

Table 3: The consequences of two methods comparing in different samples

Problems	Method	CBFs Construction(s)	Reduced Matrix Calculation(s)	Solving Matrix and RCS(s)	Total Time(s)
Problem 1	CBFM	2573.09	1910.68	24.92	4533.61
	CBFM-SVD	1519.02	1593.64	21.60	3155.86
Problem 2	CBFM	3205.64	2241.91	29.84	5507.23
	CBFM-SVD	1956.62	1797.64	22.84	3798.30
Problem 3	CBFM	3966.63	4299	41.57	8348.85
	CBFM-SVD	2607.51	3524.17	34.20	6200.08

REFERENCES

[1] R. F. Harrington, *Field Computation by Method of Moments*. IEEE Press, New York, NY, USA, 1992.

[2] R. Coifman, V. Rokhlin, and S. Wandzura, "The fast multipole method for the wave equation: A pedestrian prescription," *IEEE Antennas and Propagation Magazine*, vol. 53, no. 3, pp. 7-12, 1993.

[3] E. Bleszynski, M. Bleszynski, and T. Jaroszewicz, "Adaptive integral method for solving large-scale electromagnetic scattering and radiation problems," *Radio Science*, vol. 31, no. 5, pp. 1225-1251, 1996.

[4] J. M Song, C. C. Lu, and W. C. Chew, "Multilevel fast multipole algorithm for electromagnetic scattering by large complex objects," *IEEE Trans. Antennas Propag.*, vol. 45, no. 10, pp. 1488-1493, 1997.

[5] K. Zhao, M. N. Vouvakis, and J.-F. Lee, "The adaptive cross approximation algorithm for accelerated method of moments computations of EMC," *IEEE Transactions on Electromagnetic Compatibility*, vol. 47, no. 4, pp. 763-773, 2005.

[6] A. Freni, P. De Vita, P. Pirinoli, *et al.*, "Fast-factorization acceleration of MoM compressive domain-decomposition," *IEEE Trans. Antennas Propag.*, vol. 59, no. 1 2, pp. 4588-4599, 2011.

[7] J. Hu, R. Zhao, M. Tian, *et al.*, "Domain decomposition method based on integral equation for solution of scattering from very thin conducting cavity," *IEEE Trans. Antennas Propag*., vol. 62, no. 10, pp. 5344-5348, 2014.

[8] X. Chen, C. Gu, Z. Niu, Y. Niu, and Z. Li, "Fast dipole method for electromagnetic scattering from perfect electric conducting targets," *IEEE Trans. Antennas Propag*., vol. 60, no. 2, pp. 1186-1191, 2012.

[9] A. Schroder, H. D. Bruxns, and C. Schuster, "A hybrid approach for rapid computation of two-dimensional monostatic radar cross section problems with the multilevel fast multipole algorithm," *IEEE Trans. Antennas Propag*., vol. 60, no. 12, pp. 6058-6061, 2012.

[10] X. M. Pan and X. Q. Sheng, "Fast solution of linear systems with many right hand sides based on skeletonization," *IEEE Antennas Wireless Propag. Lett.*, vol. 15, no. 1, pp. 301-304, 2016.

[11] X. M. Pan, S. L. Huang, and X. Q. Sheng, "Wide angular sweeping of dynamic electromagnetic responses from large targets by MPI parallel skeletonization," *IEEE Trans. Antennas Propag.*, vol. 66, no. 3, pp. 1619-1623, 2018.

[12] E. Lucente, A. Monorchio, and R. Mittra, "An

iteration free MoM approach based on excitation independent characteristic basis functions for solving large multiscale electromagnetic scattering problems," *IEEE Trans. Antennas Propag*., vol. 56, no. 4, pp. 999-1007, 2008.

[13] V. V. S. Prakash and R. Mittra, "Characteristic basis function method: A new technique for efficient solution of method of moments matrix equations," *Microwave and Optical Technology Letters*, vol. 36, no. 2, pp. 95-100, 2003.

[14] Y. F. Sun, K. Lu, and G. H. Wang, "Analysis of electromagnetic scattering from dielectric objects using multilevel characteristic basis function method," *Chinese Journal of Radio Science*, vol. 28, no. 1, pp. 92-96, 2009.

[15] E. Garcia, C. Delgado, L. Lozano, I. Gonzalez-Diego, and M. F. Catedra, "An efficient hybrid-scheme combining the characteristic basis function method and the multilevel fast multipole algorithm for solving bistatic RCS and radiation problems," *Progress In Electromagnetics Research B*, vol. 34, pp. 327-343, 2011.

[16] T. Tanaka, Y, Inasawa, Y, Nishioka, and H. Miyashita, "Improved primary characteristic basic function method for monostatic radar cross section analysis of specific coordinate plane," *IEICE Transactions on Electronics*, vol. E99-C, no. 1, pp. 28-35, 2016

[17] G. Bianconi, C. Pelletti, and R. Mittra, "A high-order characteristic basis function algorithm for an efficient analysis of printed microwave circuits and antennas etched on layered media," *IEEE Antennas Wireless Propag. Lett.*, vol. 12, no. 12, pp. 543-546, 2013.

[18] Z. G. Wang, Y. F. Sun, and G. H. Wang, "Analysis of electromagnetic scattering from perfect electric conducting targets using improved characteristic basis function method and fast dipole method," *J. Electromagn. Waves Appl*., vol. 28, no. 7, pp. 893-902, 2014.

[19] K. Konno and Q. Chen, "The numerical analysis of an antenna near a dielectric object using the higher order characteristic basis function method combined with a volume integral equation," *IEICE Transactions on Communications*, vol. E97-B, no. 10, pp. 2066-2073, 2014.